# MAHLI on Mars: Lessons learned operating a geoscience camera on a landed payload robotic arm

**R. A. Yingst,[1] K. S. Edgett[2], M. R. Kennedy[2], G. M. Krezoski[2], M. J. McBride[2,3], M. E. Minitti[1], M. A. Ravine[2], and R. M. E. Williams[1]**

[1]{Planetary Science Institute, Tucson, Arizona}

[2]{Malin Space Science Systems, San Diego, California}

[3]{Now at Purdue University, West Lafayette, Indiana}

Correspondence to: R. A. Yingst (Yingst@psi.edu)

## Abstract

The Mars Hand Lens Imager (MAHLI) is a 2-megapixel, color camera with resolution as high as 13.9 μm/pixel. MAHLI has operated successfully on the martian surface for over 1150 martian days (sols) aboard the Mars Science Laboratory (MSL) rover, Curiosity. During that time MAHLI acquired images to support science and science enabling activities, including rock and outcrop textural analysis; sand characterization to further the understanding of global sand properties and processes; support of other instrument observations; sample extraction site documentation; range-finding for arm and instrument placement; rover hardware and instrument monitoring and safety; terrain assessment; landscape geomorphology; and support of rover robotic arm commissioning. Operation of the instrument has demonstrated that imaging fully illuminated, dust-free targets yields the best results, with complimentary information obtained from shadowed images. The LEDs allow satisfactory nighttime imaging but do not improve daytime shadowed imaging. MAHLI's combination of fine-scale, science-driven resolution, RGB color, ability to focus over a large range of distances, and relatively large FOV, have maximized the return of science and science-enabling observations given the MSL mission architecture and constraints.

## 1 Introduction

Operating > 1150 sols on the martian surface, the Mars Hand Lens Imager (MAHLI), aboard the Mars Science Laboratory (MSL) *Curiosity* rover, has been used by the MSL Science

Team to interrogate geologic targets at the mm- to sub-mm scale (individual grains and grain relationships). The goal of the MAHLI science investigation is to identify and interpret lithologic and textural clues that reveal processes responsible for forming and modifying the geologic record at the rover's Gale crater field site (Edgett et al., 2012). We present here a brief overview of the MAHLI investigation activities and results from the first 1150 sols, and the key lessons learned in operating this instrument.

## 2 Instrument

MAHLI is a 2-megapixel~~,~~ color camera with a macro lens that is able to focus on targets at working distances from 2.1 cm from the camera lens~~,~~ to infinity (Edgett et al., 2012; working distance is measured from the camera ~~lens~~ to the target). The camera head is mounted on a rotatable turret at the end of *Curiosity's* robotic arm (**Fig. 1**; Anderson et al., 2012). The arm positions the camera for imaging, allowing MAHLI to attain a wide variety of perspectives both around and on the rover. Two contact sensor probes extend 1.9 cm from the front lens element, to prevent the lens from contacting the surface. MAHLI was designed to provide data salient to understanding the stratigraphy, grain-scale texture, structure, mineralogy, and morphology of geologic targets.

Textures imaged by MAHLI mimic those resolvable by a geologist's handlens. When contrasting with surrounding materials, at its highest resolution (14-18 µm/pixel), MAHLI can resolve individual grains down to coarse silt size (Edgett et al., 2015). More typically for Mars, where differences between materials are more subtle, MAHLI can distinguish individual grains of very fine sand (as defined by Wentworth (1922), > 62.5 µm diameter) from unresolvable coarse silt-sized or smaller. This is particularly important to the MSL goal of detecting environments that may once have been habitable (Grotzinger et al., 2012), as mudstone is a great preserver of biosignatures.

The instrument also includes four white light and two ultraviolet (365 nm) LEDs to illuminate targets when warranted. White light LED pairs can be commanded together or separately so targets can be illuminated from multiple directions. MAHLI onboard data processing includes a ~~focus~~ merge (z-stacking) capability and lossless and lossy data compression options. Comprehensive details on the design and operation of MAHLI are in Edgett et al., 2015.

## 3 Summary of MAHLI activities

During its Primary Mission (August 2012 – September 2014), Curiosity operated on Aeolis Palus, a lowland in northern Gale between the crater's north wall and a 5-km-high mountain of stratified rock, Aeolis Mons (known informally as Mt. Sharp). Since September 2014, the rover has been investigating rocks exposed on the lowermost northern flank of Aeolis Mons. The area explored consists largely of thinly mantled to bare outcrops of wind-eroded sedimentary rock. Many of these were mafic fluvial sandstones and conglomerates, while others were siltstones and mudstones (Williams et al., 2013; Grotzinger et al., 2013; Grotzinger et al., 2015). Eolian bedforms, usually of centimeters to decimeters height, were also encountered. Examples of images of geologic targets acquired by MAHLI, over a range of scales, are shown in **Fig. 2-3**.

Typical MAHLI images of rock, regolith, and eolian targets included color images, ~~focus~~ stacks, and stereo pairs. The first science-driven imaging sequence on a rock target was was designed to provide context images for higher-resolution images (100 µm/pxl), images at scales comparable to the Mars Exploration Rovers Microscopic Imagers (31 µm/pxl) to allow for direct comparison, and highest resolution images (16-22 µm/pxl). Each of these ~~resolution~~s required a different position of the robotic arm (stand-off distance). An additional image at 31 µm/pxl (5 cm distance) was also acquired at a ~~slight~~ offset from the first to provide stereo; this resolution was chosen for stereo pairs because it was close enough to provide a good estimate of microtexture, but far enough away to be considered less risky to attempt than a closest approach (and thus best resolution) would be. Because every imaging sequence must be vetted multiple times, each change in an imaging sequence adds complexity and thus significant time to the planning cycle. As a result, this grouping of three ~~resolutions~~ quickly became the typical observational sequence used when acquiring images of science targets. These image stand-off distances were chosen early in the mission, but their usefulness has led to their being retained largely unchanged up to the present time. This "standard" sequence is shown in **Fig. 3**.

The images and other vital science and science-enabling observations enabled by the field of view and focus of the camera include:

(1) grain-scale rock textural analysis (e.g., grain size, shape, rounding, voids) which contributed to interpretations regarding rock type, facies, and diagenetic conditions (e.g., Grotzinger et al., 2013; Stack et al., 2014; Grotzinger et al., 2015) (**Fig. 2-3**);

(2) examination of eolian sand deposits, which informed a global understanding of fundamental properties and processes of eolian transport and bedform stabilization when compared to similar features at other Mars rover sites (e.g., Minitti et al., 2013; Sullivan et al., 2104; **Fig. 4**);

(3) images for the arm engineers to make lateral adjustments, based on a contextual-resolution MAHLI image taken on a prior sol (Minitti et al., 2013; Yingst et al., 2014a), and quantitative measurements to support placement of the rover's APXS, drill and scoop (**Fig. 5**; Robinson et al., 2013);

(4) sample extraction site documentation, including rover self-portraits to provide context (**Fig. 2**);

(5) imaging of rover wheels to assess and monitor damage (**Fig. 6**), as routine imaging of the wheels ~~relatively early in the mission~~ revealed a much larger number of damage points than had been previously seen over a similar distance (Yingst et al., 2014b);

(6) consistent documentation of APXS analysis spots to support interpretation of geochemical data across multiple rover sites (**Fig. 7**);

(7) imaging in support of robotic arm operation and the second phase of rover commissioning during sols 32-37, to validate the behavior of the arm under martian conditions (**Fig. 8**; Robinson et al., 2013);

(8) observations of landscape geomorphology (**Fig. 9**) and airborne dust;

(9) imaging of other instrument hardware (e.g., the MAHLI and APXS calibration targets, the CheMin inlet funnel, the SAM tunable laser spectrometer (TLS), the Rover Environmental Monitoring System (REMS) ultraviolet (UV) sensor and the ChemCam remote warm electronics box (RWEB)) to support their safety and health (Blake et al., 2012; Edgett et al., 2012; Gómez-Elvira et al., 2012, Wiens et al., 2012; Campbell et al., 2014; **Fig. 10-12**); and

(10) observations of the properties and configuration of eolian dust that settled on natural and rover hardware surfaces (**Fig. 12**).

## 4 Image scale and range finding

MAHLI image scale, for targets at working distances of 2.1 to 210 cm, is related directly to the instrument's stepper motor count. This relationship was empirically determined by measuring features of known scale, at known distance, on both Earth and Mars (Edgett et al., 2015). When the dust cover is open (which is the nominal operation mode on Mars because the dust cover was coated with a film of dust during the rover's terminal descent), the relationship between motor count ($m_{open}$) and working distance ($w$, in cm) is expressed as follows:

$$w = (a\, m_{open}^{-1} + b + c\, m_{open} + d\, m_{open}^{2} + e\, m_{open}^{3})^{-1} \quad (1)$$

in which a = 0.576786, b = -11.8479, c = 2.80153x10$^{-3}$, d = -2.266488x10$^{-7}$, and e = 6.26666x10$^{-12}$.

The relation between working distance ($w$, in cm) and the width of the area covered by each MAHLI square pixel ($p$, in µm), assuming the target is in focus ~~and is~~ a plane parallel to the camera's CCD, is:

$$p = 6.9001 + 3.5201w \quad (2)$$

Equations (1) and (2), used together, determine the pixel scale of any given image acquired by MAHLI at working distances from 2.1 to 210 cm. Equation (1) can also be used to determine the distance of the camera, and thus the robotic arm, from a target imaged by MAHLI (range finding). This capability supports precise and repeatable placement of the robotic arm, and was employed to place the robotic arm scoop for sampling of the Rocknest sand shadow eolian feature on Sols 60-89 (Minitti et al., 2013). Depth of field (DOF) contributes to uncertainty in the relation between working distance, motor count, and pixel scale. Depth of field ($d_{near}$ and $d_{far}$) increases with increasing working distance, and is determined by:

$$d_{near} \text{ or } d_{far} = (a m_{open}^{-1} + b + c m_{open} + d m_{open}^{2} + e m_{open}^{3})^{-1}, \quad (3)$$

in which, for $d_{near}$, a = 1.03565, b = –11.9083, c = 2.82403×10$^{-3}$, d = –2.29003×10$^{-7}$, and e = 6.34332×10$^{-12}$; and, for $d_{far}$, a = 1.03438, b = –11.4118, c = 2.69297×10$^{-3}$, d = –2.17752×10$^{-7}$, and e = 6.02494×10$^{-12}$ (Edgett et al., 2015).

## 5 Data distribution

MAHLI data and data products are archived with the NASA Planetary Data System (PDS) according to a release schedule determined by the MSL Project and NASA PDS. As of 4 December 2015, all data *received* as of Sol 1062 (2 August 2015) have been validated and archived; this includes all MAHLI images acquired during interplanetary cruise and pre-launch testing. In addition to the NASA PDS archives, all MAHLI images are placed online, typically < 1 hour after receipt on Earth, on a public web site maintained by the MSL Project at the California Institute of Technology's Jet Propulsion Laboratory. For MAHLI images that arrive on Earth as JPEG-compressed products, the actual as-received JPEG is placed online; for data received with lossless or no compression, the data are color-interpolated, saved as a JPEG with compression quality 95/100, and then placed online; these practices ensure the public immediately receives the highest quality JPEGs. This approach differs, in detail, from data immediately released by most other planetary instruments.

## 6 Lessons learned during operations

MAHLI has performed nominally on Mars. Here we discuss the lessons learned through 1150 sols of operation, or approximately three Earth years.

### 6.1 Operations lessons learned

#### 6.1.1 Use limitations

After a major scientific campaign exploring the lacustrine setting at Yellowknife Bay (Grotzinger et al., 2013), Curiosity's primary goal was to reach the geological targets on Aeolis Mons (Mt. Sharp). This focus on driving limited the nature and extent of all science observations during the traverse to Mt. Sharp, but in particular limited use of the robotic arm given the significant time and power resources its deployment requires. Because fulfilling MAHLI's full science investigation requires arm deployment to acquire targeted MAHLI images, MAHLI observations were largely limited to a few strategically-planned stopping points along the traverse for high-priority science (Vasavada et al 2014). As a consequence, the camera was commonly used only when another science investigation or engineering need required it; of necessity, the MAHLI science investigation alone was rarely the driving force.

Even in instances when resources allow arm, and thus MAHLI, deployment, MAHLI images are often acquired of targets that are ~~avail~~able, rather than targets that are scientifically optimal. After Curiosity arrives at an end-of-drive position and the stability of the rover for arm deployment is confirmed, constraints on positioning the 5 degree of freedom, 2.25 m long robotic arm and the 50 kg, 60 cm diameter instrument turret on its end yield a restricted usable workspace ~2m wide and 1m deep in front of the rover. Only individual targets of interest within this workspace that are characterized as safely reachable by the arm and turret are available for imaging by MAHLI. Operational time of day constraints (which are a convolution of thermal state of rover hardware at a given time of day), power for mechanism operation and heating, rover position as a function of daytime sun position, and communications relay periods that can interrupt science data acquisition further limit the ability of MAHLI to acquire images under ideal conditions (Section 6.2). Expending extra sols to perfect rover positioning for arm placement of MAHLI at a given target has thus far been viewed too resource intensive. Finally, MAHLI use is curtailed by staffing considerations. Sufficient rover engineering staff is available only one planning day per week to plan both a drive and contact science activities within the same plan. Otherwise, the science team must choose between planning a drive or contact science in a given plan. Thus, use of MAHLI is limited to available contact science planning days or requires the sacrifice of a planned rover traverse. MAHLI use has also been limited over long weekends or holidays to avoid a situation that occurred early in a campaign in the Pahrump Hills region (that campaign is explained in more detail in Section 6.1.2), in which the arm faulted with the MAHLI dust cover open. This situation required emergency commanding sessions to close the MAHLI cover when staff was normally not available. Because such emergency tactical procedures were a significant stress on personnel and other resources, it was decided that MAHLI use would be precluded in any command situation in which a fault could result in the dust cover remaining open over multiple sols. This further limits the observations that MAHLI can acquire.

Future missions will likely continue to rely on arm-mounted imagers for micron-scale grain analysis, and all such imagers will have a similar limitation. One candidate solution for mitigating this limitation would be for the mission to include an additional camera (mast-mounted) that acquires similar high-quality, high resolution images without the need for arm motion; such images would be used to prioritize candidate contact science targets, including those for higher-resolution, arm mounted camera viewing (e.g, MAHLI) (Yingst et al., 2014b).

### 6.1.2 Optimizing target selection and imaging

In part to overcome the operational challenges of acquiring science-driven MAHLI images and increase the amount of grain-scale data acquired at a particularly science-rich site informally called Pahrump Hills (Grotzinger et al., 2015), the science team designed and executed a “walkabout-first” strategy begun around sol 750, in which the rover first explored the site with its remote sensing instruments, then used these data to downselect the best sites for more detailed, time- and resource-consuming interrogation by MAHLI and other contact instruments. This strategy, commonly used in terrestrial settings, was also used during Opportunity’s examination of Whitewater Lake (Arvidson et al., 2014). This is in comparison to the linear approach commonly employed for rover fieldwork, where the rover rarely backtracks, but instead examines all sites in the order encountered (e.g., Columbia Hills and Home Plate at the Spirit site (Arvidson et al., 2007), Endurance Crater at the Opportunity landing site (Grotzinger et al., 2005), and the Kimberley region by Curiosity (Grotzinger et al., 2014; these two methods are summarized in Yingst et al., 2015). The quantitative result of this operational strategy was 198 MAHLI science targets imaged between Sols 753 and 948, compared to 478 MAHLI science targets imaged during the rest of the mission. Put another way, the Pahrump Hills MAHLI science image set represents 41% of all MAHLI science-driven images up to Sol 1100. Qualitatively, Pahrump Hills remains the only location on Mars where more than ten vertical meters of sedimentary layers have been documented and analyzed at the handlens-scale (µm to mm). Additionally, this strategy enabled the team to park the rover in a favorable orientation for getting full sunlight on MAHLI targets of choice, something difficult to accomplish during normal operations where rover orientation is often determined by other factors (e.g., McBride et al., 2015).  But even during this period at Pahrump Hills, when grain-scale science was driving high MAHLI use, ideal science targets occasionally had to be passed up for less science-rich but more reachable targets.

Another scenario where MAHLI use can be optimized is at drill sampling locations; the processes of identifying and assessing a potential drill target, drilling the target and then delivering the sample to the geochemical suite (SAM and CheMin) requires multiple sols ~~(martian days)~~; these sols provide opportunities to identify targets of high-scientific interest (other than the drill target) and design observations (i.e., number and type of images, best time of day for illumination) for MAHLI to execute.

We recommend that for those locations studied in-depth (i.e., campaigns such as those for the areas informally known as Yellowknife Bay, and Kimberley; Grotzinger et al., 2013; Grotzinger et al, 2015), the walkabout-first strategy be utilized where possible to maximize MAHLI science return. For those locations where the walkabout-first strategy is not desirable or feasible, we recommend strategically developing a robust set of science-driven criteria for MAHLI targets at each location, and a plan for reaching them (via arm motion and rover drive positioning) that is on par with, as well as in accord with, the needs of the other onboard science instrument investigations.

### 6.1.3 Terminal descent plume

Various changes in hardware configuration necessitated placing the MAHLI camera with its lens facing toward the rover's terminal descent plume during landing. The engines mobilized sand and dust, as witnessed by the rover's descent imager (Schieber et al. 2013), some of which was deposited on the rover hardware. While the MAHLI dust cover and camera head survived Curiosity's descent to the martian surface, the capability of the camera to image through its transparent dust cover was lost. Further, because of this event, the first-time opening of the dust cover was delayed to add a visual inspection, using Curiosity's Mast cameras, to ensure that no deposited grains obstructed cover motion. The loss of transparency means that the MAHLI cover must be opened essentially every time an image is acquired, rather than being able to image through the cover in potentially more risky situations (for example, when a fault could result in the MAHLI cover being left open and the lens exposed to dust settling for multiple sols, or in an active dune field). Avoiding such risk has necessitated that MAHLI not be used in these situations. Future missions with similar imagers should consider avoiding an instrument accommodation in which the camera is pointed directly into the plume of dust and debris lofted by descent engines, or taking other safeguards, such as installing a deployable cover.

### 6.1.4 Stowed camera position

Between July 2013 and September 2015, MAHLI regularly acquired an image when the robotic arm was in a stowed position (**Fig. 9**), after each drive, termed an "End of Drive Stowed Image" or EDSI). These images document a portion of the landscape, in color, although the pointing is fixed (view is to the front left of the rover). Because the camera detector (CCD) mounting position inside the instrument is rotated 210° relative to the stowed position of the camera, these images are not acquired in typical "portrait" or "landscape" orientations. Serendipitously, this orientation has been found to be perfect for balancing the information content visible in the vertical and horizontal directions; sky color as a function of height can be observed, as can near-field geologic features and mid- and far-field landmarks visible in the highest resolution orbiter images. When the rover drove backwards to minimize wheel damage, these ~~terminal~~ drive images often captured rover tracks and provided parting views of the terrain that yielded added geomorphological and stratigraphic context for other MSL observations.

## 6.2 Imaging best practices

### 6.2.1 Dust free surfaces

On Earth, rain usually keeps rock outcrop surfaces clean of dust that may settle from the atmosphere. This is not the case on Mars. Dust-free surfaces are rare, but yield best results in determining lithology when imaging on Mars. Areas where wind, the rover's dust removal tool (DRT; Anderson et al., 2012) or the ChemCam Laser Induced Breakdown Spectrometer (LIBS; Wiens et al., 2012) removed the surface dust provided better science return than dust-covered surfaces (**Fig. 13**). A tool specifically designed to remove dust and provide contact instrument access to fresh rock surfaces, such as the descoped surface removal tool (SRT; Edgett et al., 2012) or a notional robotic rock hammer, would have been more beneficial. In lieu of such a tool, targets that have been disturbed by the rover or other hardware (e.g., broken rocks, disturbed dirt) can also provide cleaner or fresh surfaces, but opportunities to create and view these have been limited.

### 6.2.2 Solar illumination and shadow

Our experience shows that daytime MAHLI images of geologic materials are best acquired when the target is illuminated by sunlight, particularly with phase angles approaching 90°. This is because targets on Mars in full shadow tend to appear to be more orange-brown than they actually are, and the shadowing de-emphasizes vital color and textural detail. That being said, it is ideal to acquire both fully sun-lit and fully shadowed views of the same target at the same scale, because both provide information that the other does not provide alone. Fully illuminated targets yield the best natural color and textural information to discern individual grains, characterize grain morphology, and identify subtle geologic features, while applying the dynamic range of the camera to a fully shadowed scene yields a scene with greater contrast, and thus a greater discrimination between subtle color differences. These differences can be seen in **Fig. 14**. Images acquired in partial sunlight have proven to be least useful, as both of these advantages are lessened. Specifically, such a mixed image provides less of the target in full illumination, and stretching the shadowed portion of the image is less effective as a fully shadowed image.

### 6.2.3 Artificial illumination source

When using an artificial light source, phase angle can reduce apparent depth, which in turn lessens textural heterogeneity and challenges autofocus; MAHLI's white light LEDs are at different positions that can operate independently (Edgett et al., 2012), which provides shadowing, lessening this problem. When imaging at night, the placement of the LEDs is adjusted to create the best image. When imaging a drill hole, for example, one set of LEDs is pointed directly into the hole. Though it did not improve image quality when used to illuminate shadowed targets during daytime or twilight, under Mars conditions, the LEDs provided effective illumination of target color and texture under nighttime conditions (Minitti et al., 2014). This is thus an important capability, as it increases the number of MAHLI imaging opportunities by permitting the acquisition of MAHLI images without delaying other activities that require daylight (e.g., driving). Thus, while the preferred illumination conditions are daytime full sunlight or shadow, the LEDs have significantly increased useful MAHLI image acquisition.

### 6.2.4 Focus range and field of view

The relatively large field of view (FOV) of MAHLI (38.5° diagonal at infinity focus), and its ability to focus over a large range of working distances, were key capabilities that permitted crucial science-enabling rover and instrument hardware engineering observations, including imaging the rover wheels to identify and monitor damage (**Fig. 6**; Yingst et al., 2014b); monitoring of other instruments for dust accumulation; imaging inside the laboratory inlets (e.g., SAM, CheMin) for sample cross-contamination (**Fig. 10**); and contributing to diagnosis or better understanding of other hardware problems (e.g., damage on REMS boom 1, ChemCam mirror dust accumulation; **Fig. 11**). Many of these observations are now acquired at a standard cadence for routine health and safety checks of the hardware and instruments. A smaller FOV would have resulted in significantly more images being necessary for each of these crucial imaging activities (and thus more time and rover resources), potentially limiting the ability of the team to monitor and protect the instruments and the rover. For example, MAHLI wheel imaging originally included a six image sequence with an image manually focused on each wheel; however, the two dedicated middle wheel images were dropped starting on sol 587 as extraneous, because the relatively large FOV allowed all wheels to be imaged using only four images. Additionally, ~~it~~ has been able to produce mosaics that show the entire rover in field context (**Fig. 2**), using 2–3x fewer images than would a similar camera with a resolution of 7–8 µm/pxl (and correspondingly narrower FOV). This translates to significantly less time spent on engineering and housekeeping activities, and thus more time and resources that can be devoted to science-driven activities. Future landed missions (e.g., Moon, Mars, small bodies) should consider the benefits of utilizing a high-fidelity arm-mounted camera with a large FOV and focus range to support engineering diagnostic concerns, both seen and unforeseen.

## 7 Conclusions

MAHLI has proven to be robust, efficient in operation, and flexible in the images and derivative products it yields. The combination of fine-scale resolution, RGB color, ability to focus over a large range of distances, and relatively large FOV, have provided maximum science and science-enabling return given the MSL mission architecture and constraints. Resolution down to coarse silt allows discrimination among potential habitable environments (mudstone versus sandstone, for example) without greatly increasing focal length, and thus mass and volume. Color has proven to be a crucial discriminator among sedimentary grains of a similar morphology, fabric or sorting, but different lithologies. This has been especially true for fine-grained rock targets, where very subtle color differences are in some cases one of the only ways to determine grain boundaries. The ability to determine the relationship between the variable focus stepper motor count and distance to the lens allows MAHLI to be used for range finding for robotic arm placement if a target has been approached once.

Finally, the MAHLI optical configuration strikes a very favorable balance between resolution and FOV, enabling images from grain to rover to landscape-scale. Owing to this balance, an increase in spatial resolution of a future MAHLI-like instrument would yield only a marginal improvement in overall science return.

## Author contributions

R. A. Yingst, K. S. Edgett, M. J. McBride, M. E. Minitti and R. M. E. Williams contributed significant analysis to the reported science results. M. A. Ravine led the effort to build the instrument and M. R. Kennedy, G. M. Krezoski and M. E. Minitti led the operations efforts, with assistance from R. A. Yingst and K. S. Edgett. All authors contributed to the conception, development, execution and further refinement of MAHLI operational sequences. R. A. Yingst prepared the manuscript with contributions from all co-authors.


## Acknowledgements

We gratefully acknowledge all the individuals who have made MAHLI operations a success: the MAHLI Payload Uplink and Downlink Leads, Data Management leads, and all the engineers at JPL responsible for operating the rover arm. The authors also wish to thank the reviewers, whose comments improved this manuscript. This work was supported by the Mars Science Laboratory Program through Malin Space Science Systems contract 08-0315 to R.A.Y.

## References

Anderson R. C., Jandura, L., Okon, A. B., Sunshine, D., Roumeliotis, C., Beegle, L. W., Hurowitz, J., Kennedy, B., Limonadi, D., McCloskey, S., Robinson, M., Seybold, C., and Brown, K., Collecting samples in Gale Crater, Mars: an overview of the Mars Science Laboratory Sample Acquisition, Sample Processing and Handling System, Space Sci. Rev. 170, 57–75, doi:10.1007/s11214-012-9898-9, 2012.

Arvidson, R. E., et al., Spirit's campaign in the inner basin, Columbia Hills, Gusev Crater, Lunar Planet Sci. Conf. 38$^{th}$, Abs. #1122, 2007.

Arvidson, R.E., et al., Ancient aqueous environments at Endeavour crater, Mars, Science, 343, 1248097, 2014.

Berger J. A., King, P. L., Gellert, R., Campbell, J. L., Boyd, N. I., Pradler, I., Perrett, G. M., Edgett, K. S., VanBommel, S. J. V., Schmidt, M. E., and Lee, R. E. H., MSL-APXS titanium observation tray measurements: Laboratory experiments and results fort he rocknest fines at the Curiosity field site in Gale Crater, Mars, J. Geophys. Res. 119(5), 1046–1060, doi:10.1002/2013JE004519, 2014.

Blake D. F., Morris, R. V., Kocurek, G., Morrison, S. M., Downs, R. T., Bish, D., Ming, D. W., Edgett, K. S., Rubin, D., Goetz, W., Madsen, M. B., Sullivan, R., Gellert, R., Campbell, I., Treiman, A. H., McLennan, S., M., Yen, A. S., Grotzinger, J., Vaniman, D. T., Chipera, S. J., Achilles, C. N., Rampe, E. B., Sumner, D., Meslin, P. –Y., aurice, S., Forni, O., Gasnault, O., Fisk, M., Schmidt, M., Mahaffy, P., Leshin, L. A., Glavin, D., Steele, A., Freissinet, C., Navarro-González, R., Yingst, R. A., Kah, L. C., Bridges, N., Lewis, K. W., Bristow, T. F., Farmer, J. D., Crisp, J. A., Stolper, E. M., Des Marais, D. J., Sarrazin, P., and the MSL Science Team, Curiosity and Gale Crater, Mars: Characterization and analysis of the Rocknest sand shadow, Science, 341, doi:10.1126/science.1239505, 2013.

Campbell, J. L., King, P. L., Burkemper, L., Berger, J. A., Gellert, R., Boyd, N. I., Perrett, G. M., Pradler, I., Thompson, L., Edgett, K. S., and Yingst, R. A., The Mars Science Laboratory APXS calibration target: Comparison of Martian measurements with the terrestrial calibration, Nucl. Inst. Method. Phys. Res. B, 323, 49–58, doi:10.1016/j.nimb.2014.01.011, 2014.

Conrad P. G, Eigenbrode, J. L., Von der Heydt, M. O., Mogensen, C. T., Canham, J., Harpold, D. N., Johnson, J., Errigo, T., Glavin, D. P., and Mahaffy, P. R., The Mars Science

Laboratory organic check material, Space Sci. Rev. 170, 479–501, doi:10.1007/s11214-012-9893-1, 2012.

Edgett K. S., Yingst, R. A., Ravine, M. A., Caplinger, M. A., Maki, J. N., Ghaemi, F. T., Schaffner, J. A., Bell, J. F., III, Edwards, L. J., Herkenoff, K. E., Heydari, E., Kah, L. C., Lemmon, M. T., Minitti, M. E., Olson, T. S., Parker, T. J., Rowland, S. K., Schieber, J., Sullivan, R. J., Sumner, D. Y., Thomas, P. C., Jensen, E. H., Simmonds, J. J., Sengstacken, A. J., Willson, R. G., and Goetz, W., Curiosity's Mars Hand Lens Imager (MAHLI) investigation, Space Sci. Rev. 170, 259–317, doi:10.1007/s11214-012-9910-4, 2012.

Edgett, K. S., Caplinger, M. A., Maki, J. N., Ravine, M. A., Ghaemi, F. T., McNair, S., Herkenhoff, K. E., Duston, B. M., Willson, R. G., Yingst, R. A., Kennedy, M. R., Minitti, M. E., Sengstacken, A. J., Supulver, K. D., Lipkaman, L. J., Krezoski, G. M., McBride, M. J., Jones, T. L., Nixon, B. E., Van Beek, J. K., Krysak, D. J., and Kirk, R. A., Curiosity's robotic arm-mounted Mars Hand Lens Imager (MAHLI): Characterization and calibration status, *MSL MAHLI Technical Report 0001* (19 June 2015). doi:10.13140/RG.2.1.3798.5447, 2015.

Grotzinger, J. P., et al., Stratigraphy and sedimentology of a dry to wet eolian depositional system, Burns formation, Meridiani Planum, Mars, Earth and Planetary Science Letters, 240, 11-72, 2005.

Grotzinger J. P., Sumner, D. Y., Kah, L. C., Stack, K., Gupta, S., Edgar, L., Rubin, D., Lewis, K., Schieber, J., Mangold, N., Milliken, R., Conrad, P. G., Des Marais, D., Farmer, J., Siebach, K., Calef, F., III, Hurowitz, J., McLennan, S. M., Ming, D., Vaniman, D., Crisp, J., Vasavada, A., Edgett, K. S., Malin, M., Blake, D., Gellert, R., Mahaffy, P., Wiens, R. C., Maurice, S., Grant, J. A., Wilson, S., Anderson, R. C., Beegle, L., Arvidson, R., Hallet, B., Sletten, R. S., Rice, M., Bell, J., III, Griffes, J., Ehlmann, B., Anderson, R. B., Bristow, T. F., Dietrice, W. E., Dromart, G., Eigenbrode, J., Fraeman, A., Hardgrove, C., Herkenhoff, K., Jandura, L., Kocurek, G., Lee, S., Leshin, L. A., Leveille, R., Limonadi, D., Maki, J., McCloskey, S., Meyer, M., Minitti, M., Newsom, H., Oehler, D., Okon, A., Palucis, M., Parker, T., Rowland, S., Schmidt, M., Squyres, S., Steele, A., Stolper, E., Summons, R., Treiman, A., Williams, R., Yingst, A., and the MSL Science Team, A habitable fluvio-lacustrine environment at Yellowknife Bay, Gale Crater, Mars, Science, 343(6169), doi:10.1126/science.1242777, 2013.

Grotzinger, J. P., et al., A habitable fluvio-lacustrine environment at Yellowknife Bay, Gale Crater, Mars, Science, 343, 1242777, 2014.

Lee R. E., Schmidt, M. E., Gellert, R., Campbell, J. L., King, P. L., and Edgett, K. S., Linking MAHLI and APXS to analyze dust coverage on Yellowknife Bay rock targets, Lunar Planet. Sci. Conf., 45th, Abs. 2144, 2014.

McBride, M. J., Minitti, M. E., Stack, K. M., Yingst, R. A., Edgett, K. S., Goetz, W., Herkenhoff, K. E., Heydari, E., Kah, L. C., Rowland, S. K., Schieber, J., Harker, D., Kennedy, M. R., Krezoski, G. M., Lipkaman, L., Nixon, B., Van Beek, J. (2015) Mars Hand Lens Imager (MAHLI) observations at the Pahrump Hills field site, Gale crater, Lunar Planet. Science Conf., 46th, Abs. 2885, 2015.

Minitti M. E., Kah, L. C., Yingst, R. A., Edgett, K. S., Anderson, R. C., Beegle, L. W., Carsten, J. L., Deen, R. G., Goetz, W., Hardgrove, C., Harker, D. E., Herkenhovv, K. E., Hurowitz, J. A., Jandura, L., Kennedy, M. R., Kocurek, G., Krezoski, G. M., Kuhn, S. R., Limonadi, D., Lipkaman, L., Madsen, M. B., Olson, T. S., Robinson, M. L., Rowland, S. K., Rubin, D. M., Seybold, C., Schieber, J., Schmidt, M., Sumner, D. Y., Tompkins, V. V., Van Beek, J. K., and Van Beek, T., MAHLI at the Rocknest sand shadow: Science and science-enabling activities, J. Geophys. Res. 118(11), 2338–2360. doi:10.1002/2013JE004426, 2013.

Minitti M. E., Edgett, K. S., Yingst, R. A., Conrad, P.G., Fisk, M., Hardgrove, C. J., Herkenhoff, K. E., Kah, L. C., Kennedy, M. R., Krezoski, G. M., Lemmon, M. T., Lipkaman, L., Kuhn, S. R., Robinson, M. L., Tompkins, V. V., Treiman, A., and Williford, K. H., MAHLI after dark: Nighttime Mars Hand Lens Imager observations under LED illumination, Lunar Planet. Sci. Conf., 45th, Abs. 2029, 2014.

Robinson, M., Collins, C., Leger, P., Kim, W., Carsten, J., and Tompkins, V., Test and validation of the Mars Science Laboratory robotic arm, 8th International Conference on System of Systems Engineering (SoSE), doi:10.1109/SYSoSE.2013.6575264, 2013.

Schieber, J., Malin, M. C., Olson, T., Calef, F., Comeaux, K., and the MSL Science Team, The final 2 1⁄2 minutes of terror—What we learned about the MSL landing from the images taken by the MARDI descent imager, Lunar Planet. Sci. Conf., 44th, Abs. 1260, 2013.

Stack, K. M., Grotzinger, J. P., Kah, L. C., Schmidt, M. E., Mangold, N., Edgett, K. S., Sumner, D. Y., Siebach, K. L., Nachon, M., Lee, R., Blaney, D. L., Deflores, L. P., Edgar, L. A., Fairén, A. G., Leshin, L. A., Maurice, S., Oehler, D. Z., Rice, M. S., and Wiens, R. C., Diagenetic origin of nodules in the Sheepbed member, Yellowknife Bay formation, Gale crater, Mars, J. Geophys. Res,. 119(7), 1635–1664, doi:10.1002/2014JE004617, 2014.

Sullivan R., Bridges, N., Herkenhoff, K., Hamilton, V., and Rubin, D., Transverse aeolian ridges (TARs) as megaripples: Rover encounters at Meridiani Planum, Gusev, and Gale, 8th Internat. Conf. Mars, Abs. 1424, 2014.

Wentworth, C. K., A scale of grade and class terms for clastic sediments, J. Geol., 30, 377–392, doi:10.1086/622910, 1922.

Wiens R. C., Maurice, S., Barraclough, B., Saccoccio, M., Barkley, W. C., Bell, J. F., III, Bender, S., Bernardin, J., Blaney, D., Blank, J., Bouyé, M., Bridges, N., Bultman, N., Caïs, P., Clanton, R. C., Blark, B., Clegg, S., Cousin, A., Cremers, D., Cros, A., DeFlores, L., Delapp, D., Dingler, R., D'Uston, C., Dyar, M. D., Elliott, T., Enemark, D., Fabre, C. Flores, M., Forni, O., Gasnault, O., Hale, T., Hays, C., Herkenhoff, K., Kann, E., Kirkland, L., Kouach, D., Landis, D., Langevin, Y., Lanza, N., LaRocca, F., Lasue, J., Latino, J., Limonadi, D., Lindensmith, C., Little, C., Mangold, N., Manhes, G., Mauchien, P., McKay, C., Miller, E., Mooney, J., Morris, R. V., Morrison, L., Nelson, T., Newsom, H., Ollila, A., Ott, M., Pares, L., Perez, R., Poitrasson, F., Provost, C., Reiter, J. W., Roberts, T., Romero, F., Sautter, V., Salazar, S., Simmonds, J. J., Stiglich, R., Storms, S., Striebig, N., Thocaven, J., Trujillo, T., Ulibarri, M., Vaniman, D., Warner, N., Waterbury, R., Whitaker, R., Witt, J., and Wong-Swanson, B., The ChemCam instrument suite on the Mars Science Laboratory (MSL) rover: Body unit and combined system tests, Space Sci. Rev. 170, 167–227, doi:10.1007/s11214-012-9902-4, 2012.

Williams, R. M. E., et al., Martian fluvial conglomerates at Gale Crater, Science, 340(6136), 1068–1072, doi:10.1126/science.1237317, 2013.

Yingst, R. A., Edgett, K. S., Kennedy, M. R., Minitti, M. E., and Ravine, M. A., Cameras on landed payload robotic arms — MAHLI on Mars and lessons learned from one Mars year of operations, Conference on Instrumentation for Planetary Missions, Abs. 1031, 2014a.

Yingst, R. A., Hamilton, V. E., Arvidson, R., Calef, F., Grotzinger, J., Lewis, K., and Williams, R. M. E., Terrain assessment in Gale Crater from sol 0-500 using orbital thermal inertia and in situ visible data, Geol. Soc. Am. Abs., #202-8, 2014b.

Yingst, R. A., Berger, J. A., Cohen, B. A., Hynek, B. M., and Schmidt, M. E., A test of two field methods: Determining best practices in reconnoitering sites for habitability potential using a semi-autonomous rover, Lunar Planet. Sci. Conf., Abs., #1640, 2015.

**Figures.**

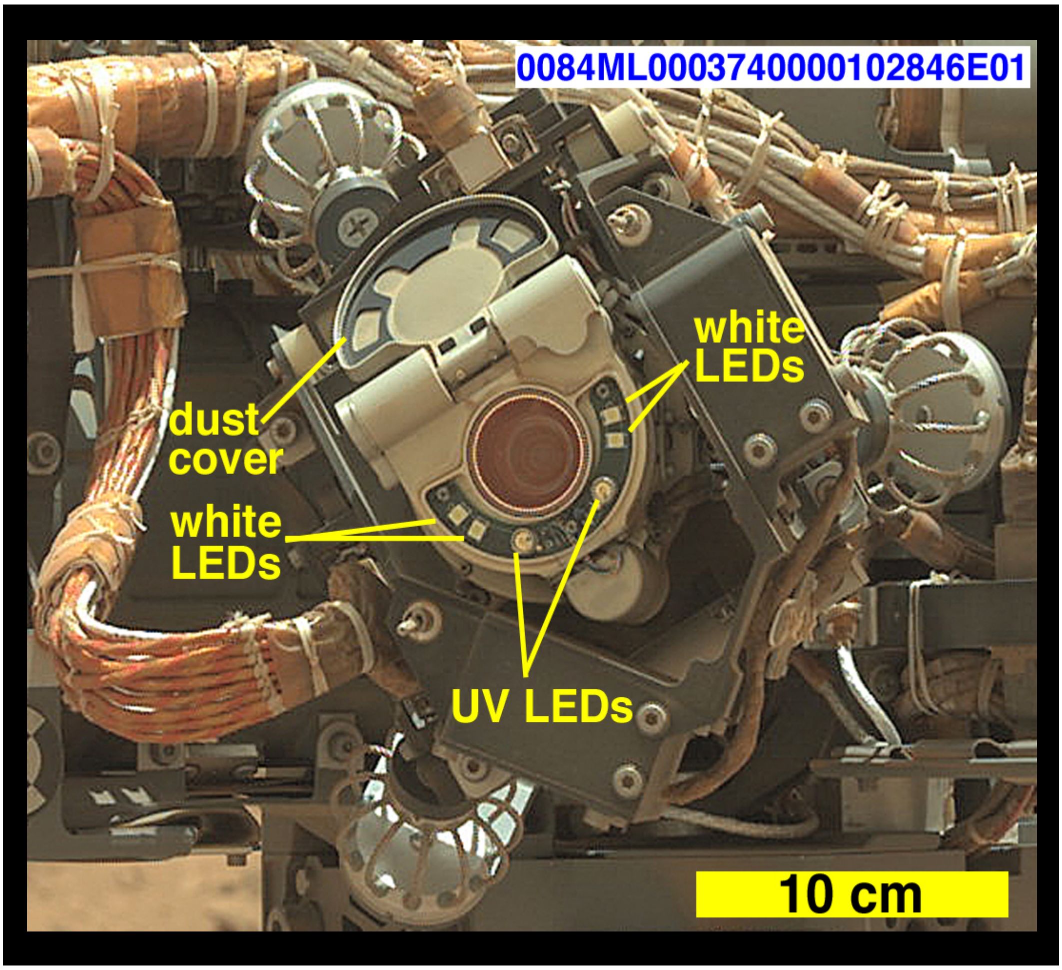


Figure 1. MAHLI camera head with dust cover open, as seen on Mars by MSL's left mast-mounted camera (Mastcam-34) on 31 Oct. 2012.

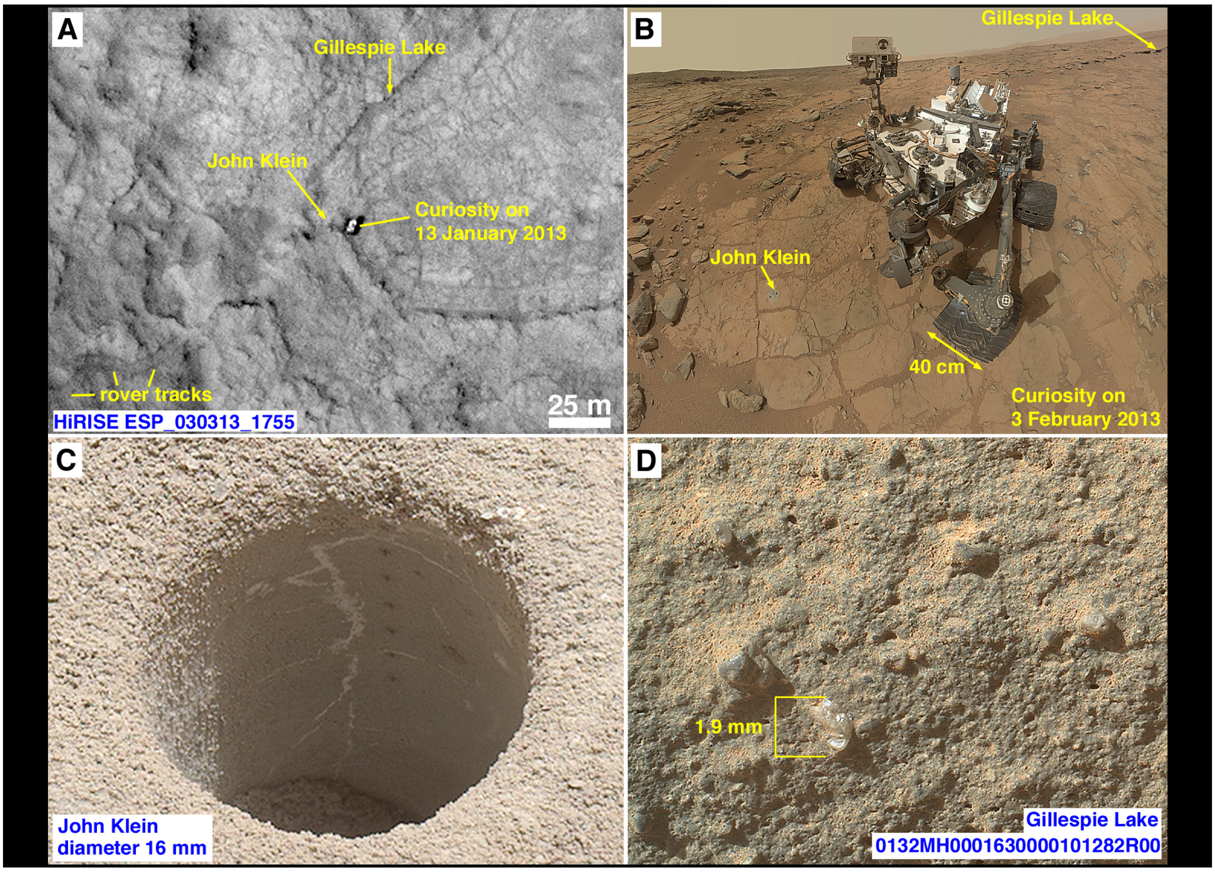


Figure 2. MSL MAHLI is designed with a combination of relatively large field of view and high resolution, allowing the camera to provide images tying orbital data down to the grain scale. Except for the HiRISE image **A**, the other pictures, here, are from MAHLI. **B** is a mosaic of MAHLI images, demonstrating MAHLI's ability to provide local context for high-resolution grain-scale images; **C** is a focus merge composite of the John Klein drill hole, with white mineralized veins and a vertical column of ChemCam LIBS spots, in the Sheepbed mudstone; and **D** is a focus merge product at highest resolution showing the gray, mafic Gillespie Lake sandstone and a single, 1.9 mm opalescent sand grain.

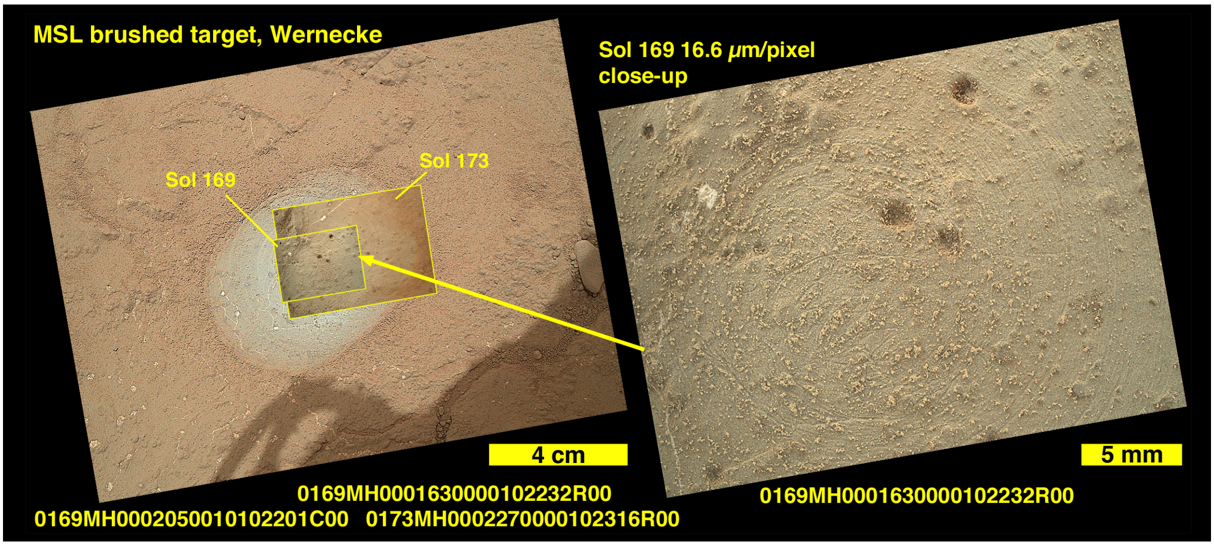


Figure 3. Sheepbed mudstone and example of nested MAHLI images of increasing spatial resolution. Left: Three MAHLI images acquired at working distances of 25, 5 and 1 cm, yielding images at 100, 31 and ~17 μm per pixel respectively. This is the most common MAHLI imaging sequence used, as it provides contextual imaging, MI-scale imaging for direct comparison to MER data, and highest, grain-scale resolution. Right: High resolution, fully-shadowed image from the nested suite, acquired at 1 cm working distance from the target.

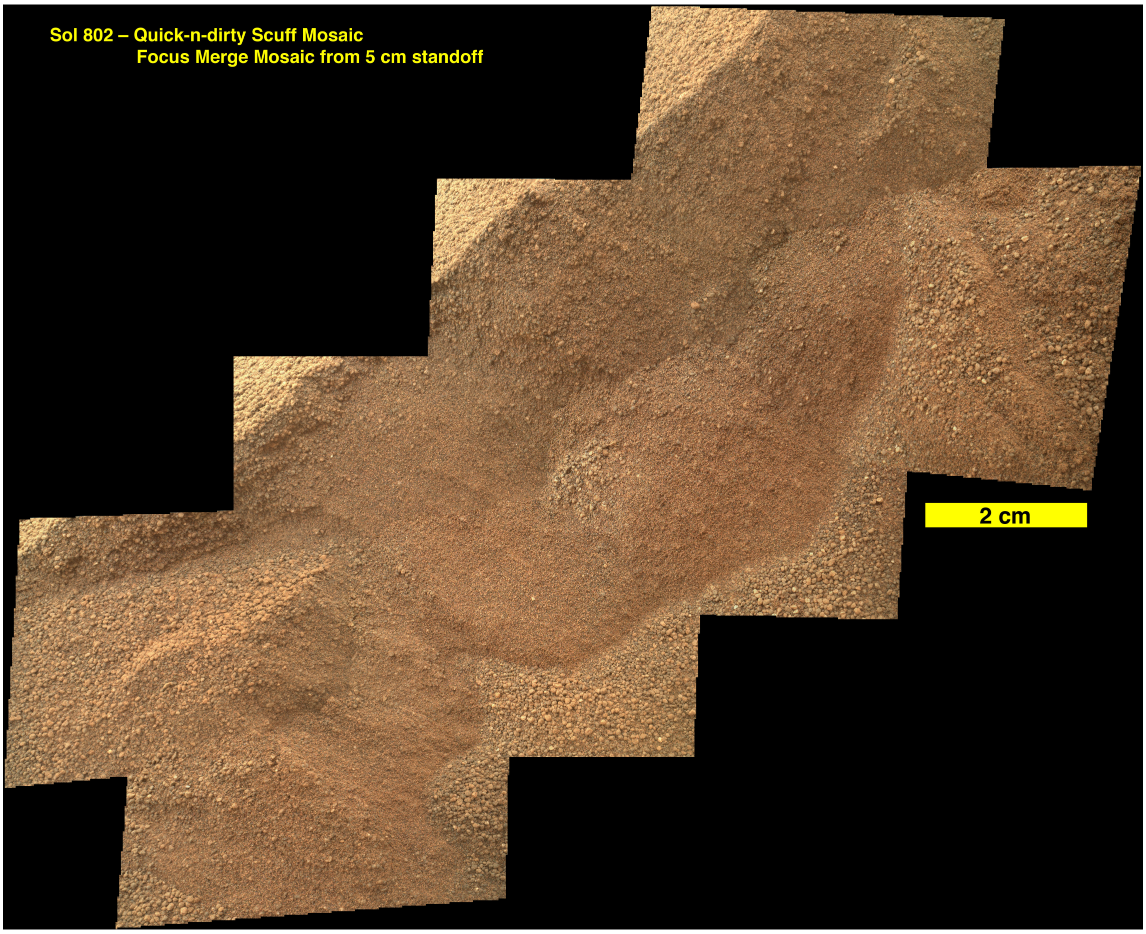


Figure 4. Mosaic of eolian sand deposits along a scuff created by the rover wheel; images acquired on sol 802. Material in the upper part of the mosaic shows the surface and interior of a megaripple (or “coarse-grained ripple”), a type of aeolian bedform that has been encountered frequently by rovers, including MSL (sometimes as a trafficability hazard). The interior of this bedform was exposed during a wheel scuff on sol 799.

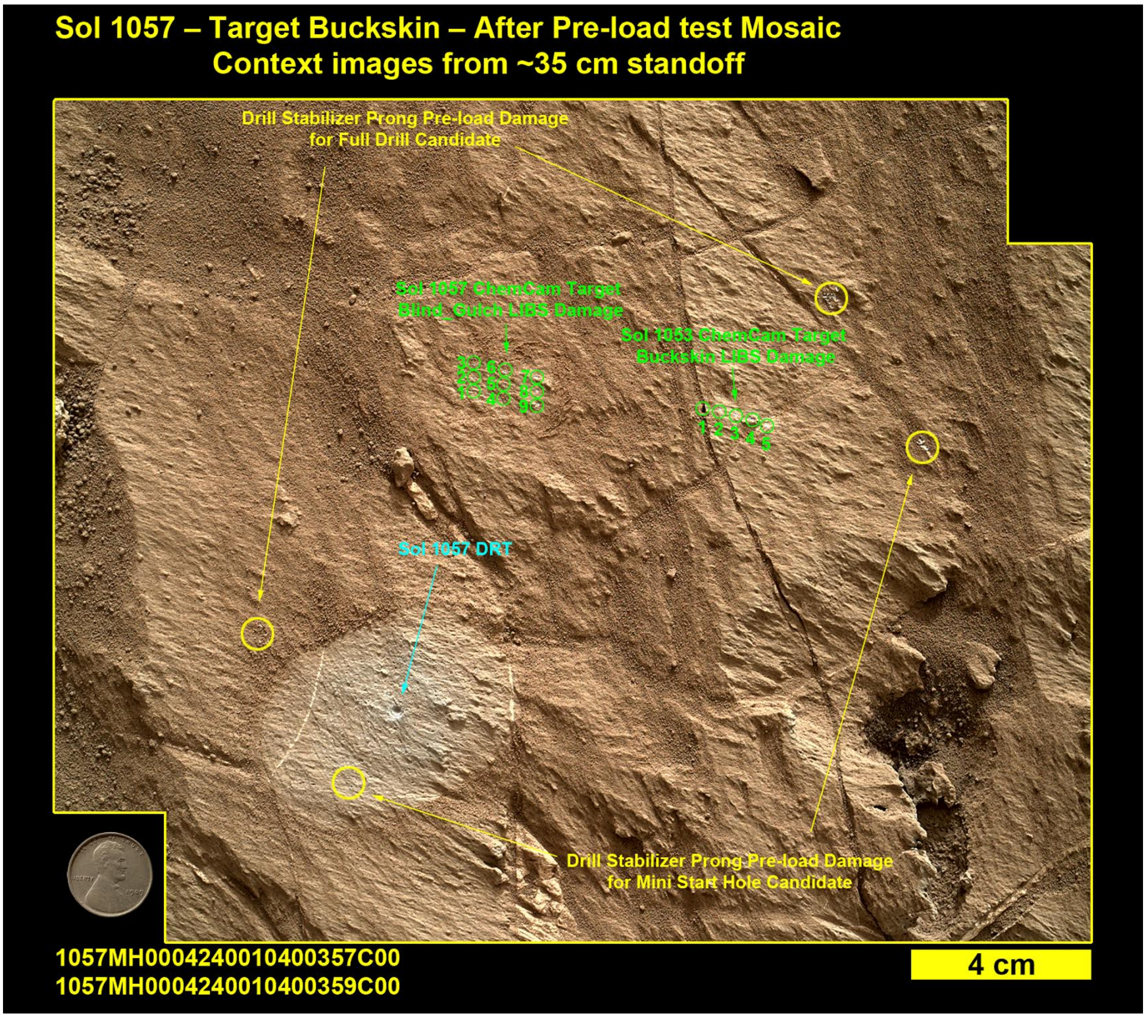


Figure 5. Image mosaic documenting placement of the drill hardware, acquired on sol 1057. Such imaging over the holes made by drill activity is commonly acquired at 35 cm distance, for more accurate placement of the drill stabilizers and drill, and for confirmation that drill activities were executed nominally and results were as expected.

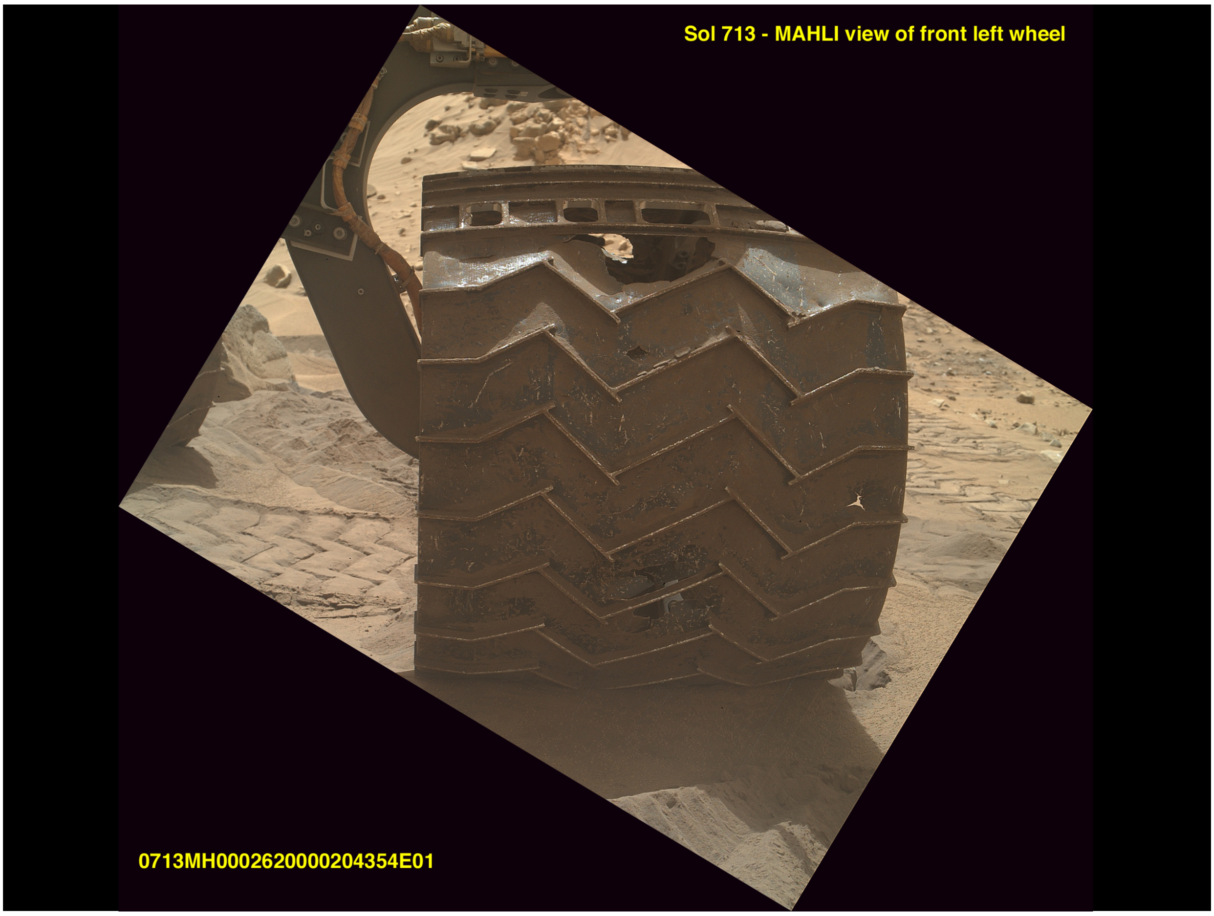


Figure 6. Example of rover wheel inspection imaging, acquired on sol 713. Wheels are 40 cm wide. Because the wheels are a non-renewable resource, MAHLI is used on a regular cadence to monitor damage; thus, Single MAHLI Wheel Imaging (SMWI), begun on sol 177, is acquired every 100 m. Full MAHLI Wheel Imaging (FMWI), begun on sol 488, is acquired every 500 m. MAHLI is also used to identify and avoid terrain that is potentially hazardous to the wheels (Yingst et al., 2014b).

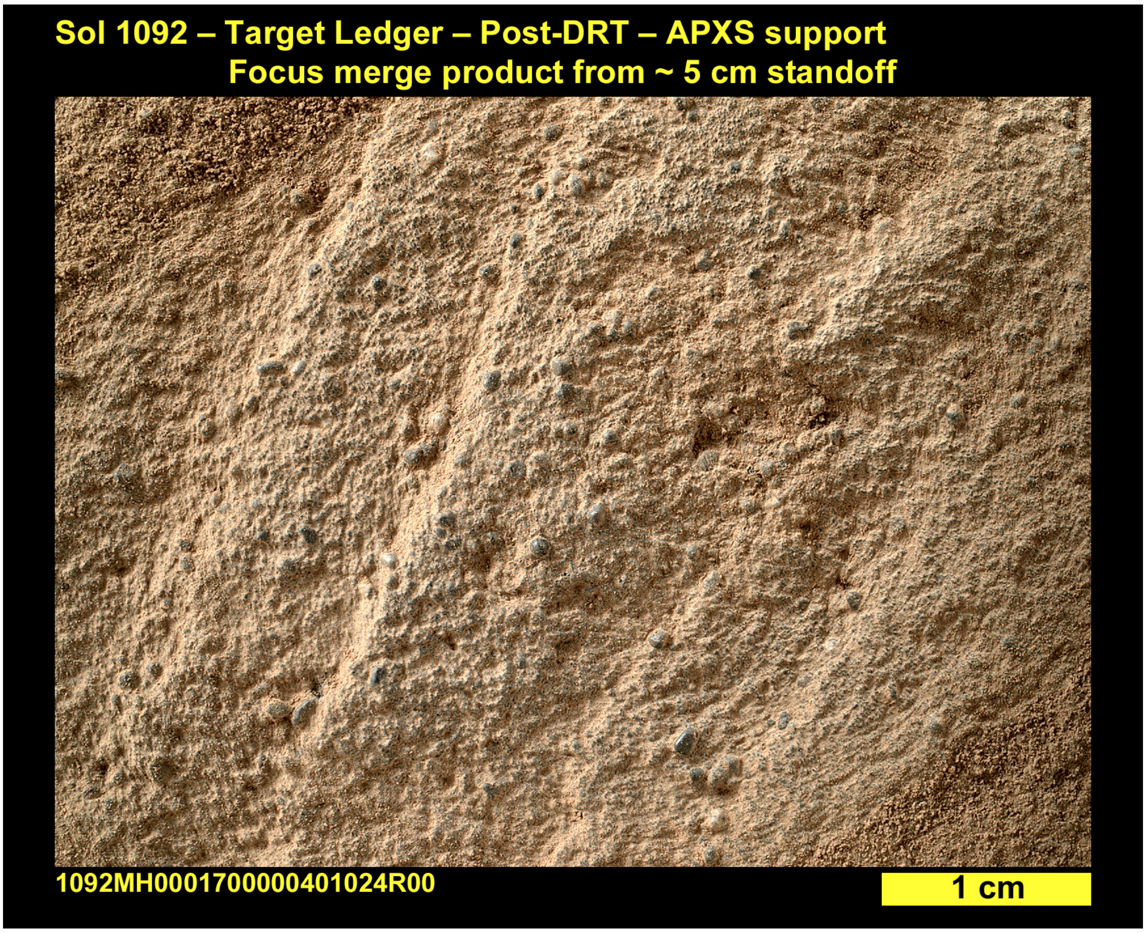


Figure 7. Image of the target Ledger acquired on sol 1092 after brushing, documenting the spot at which the APXS would collect geochemical data. MAHLI acquires images from ~7 cm working distance (field of view ~5 x 3.75 cm) at most APXS science targets; this documentation is possible because the offset between the center of a MAHLI image and the center of an APXS integration spot is 0.5-5 mm despite the instruments being positioned on opposite sides of the instrument turret (VanBommel et al., 2015). Imaging documentation has proved to be crucial in assessing the amount of dust cover influencing the chemistry of APXS integration. On targets where the dust has been mostly cleared by the Dust Removal Tool (DRT), MAHLI images record grains, veins, fractures and remnant dust that may contribute to the measured APXS chemistry.

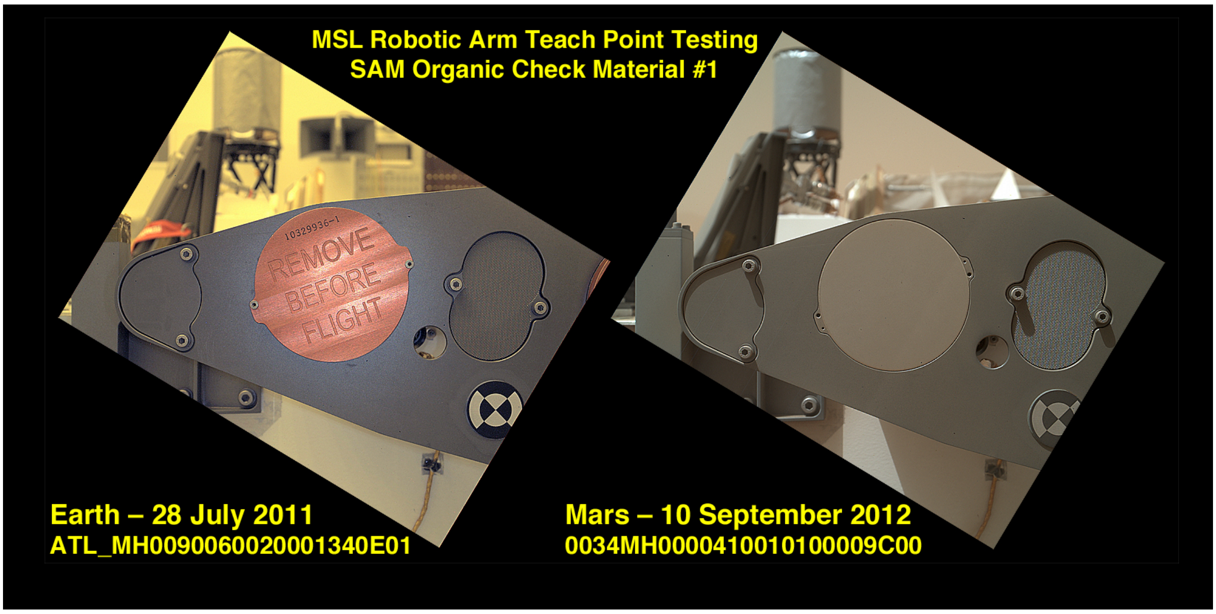


Figure 8. Example of MSL MAHLI imaging support for robotic arm teach point establishment. The Organic Check Material (OCM; circular feature) diameter is 6.25 cm (Conrad et al., 2012). During the second phase of rover commissioning (sols 32-37), MAHLI was employed to image portions of the rover to record their status post-landing, and designated arm and turret positions (teach points) over rover hardware that was expected to be imaged repeatedly over the course of the mission. These included two of the five OCMs (1 and 5; Conrad et al., 2012), one of two replacement drill bit boxes (Anderson et al., 2012), and the observation tray (Anderson et al., 2012, Berger et al., 2014).

Figure 9. Example of MAHLI view of landscape acquired on sol 634 when robotic arm was in a stowed position; this image shows the Kimberley field site and the north wall of Gale crater. Distance between right and left side wheel tracks is about 2.8 m.

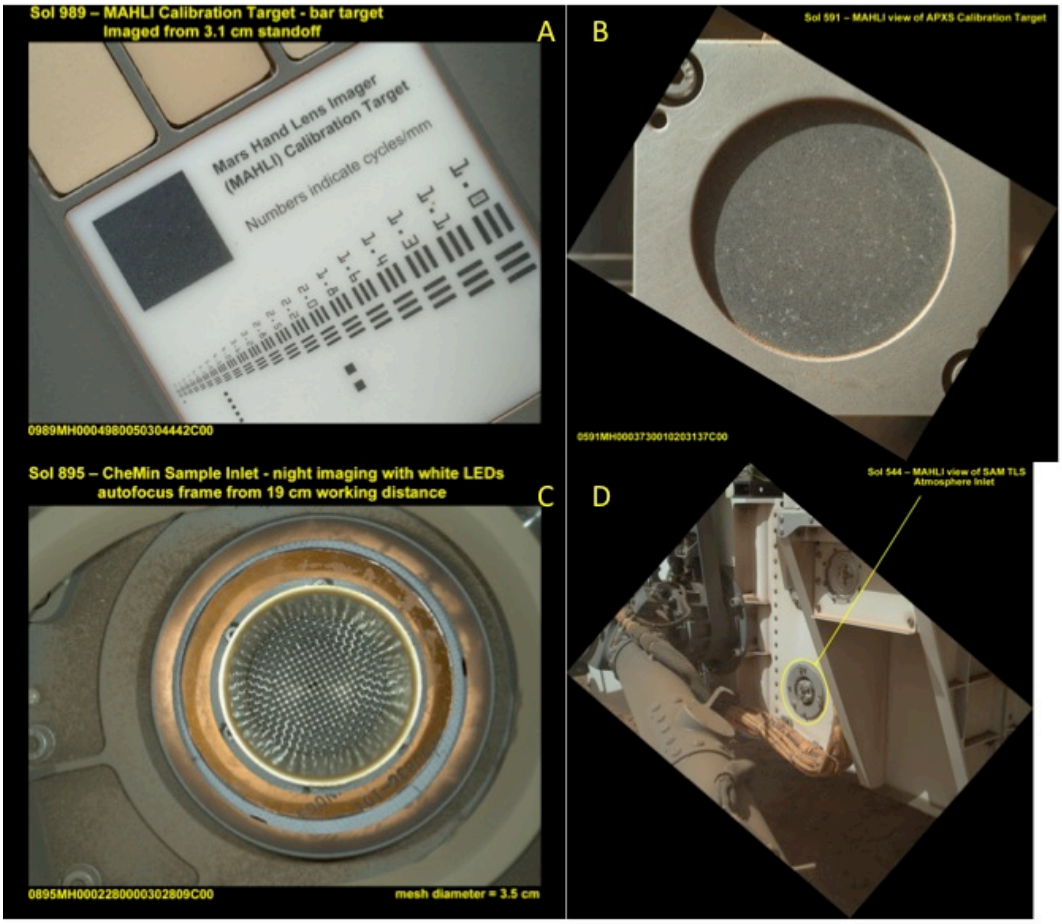


Figure 10. MAHLI images acquired of ~~several instruments~~. Such images are acquired periodically or as needed, to support instrument health and safety. **A** is a sol 989 image of a portion of the MAHLI calibration target (the full target includes the bar target seen here, as well as gray, color (RGB) and UV fluorescent swatches, stair steps and penny (Edgett et al., 2012)); this image is acquired on a 180-sol cadence to monitor camera performance. **B** is an image of the APXS calibration target acquired on sol 591 (also taken on a 180-sol cadence), to record dust cover (Campbell et al., 2014). **C** is an image acquired on sol 895 of the open CheMin sample inlet focused on the inlet funnel and on the mm-scale mesh overlying the funnel; acquired after delivery of sample to the CheMin instrument (Blake et al., 2012), this practice detects remnant material within the inlet after delivery and verifies removal of such material before the next sample delivery. **D** is a sol 544 image of the SAM tunable laser spectrometer (TLS) inlet on the starboard side of the rover chassis. Early in the mission, MAHLI supported Sample Analysis at Mars (SAM) operations by looking for evidence of disrupted sample delivery in images of both closed SAM inlet covers. As the only camera on

the rover capable of viewing it, MAHLI was utilized to look for a potential obstruction in the SAM TLS inlet.


Figure 11. Example of MAHLI image of the ChemCam window, from sol 808 (image a focus merge product, rotated so that hardware is aligned). MAHLI periodically images the window in the ChemCam RWEB, which contains the instrument's laser, telescopic optics and remote microscopic imager (RMI), to detect changes in dust contamination, and images of the fiber optic cable that carries the signal to the spectrometers within the rover body, to look for cable wear (Wiens et al., 2012).

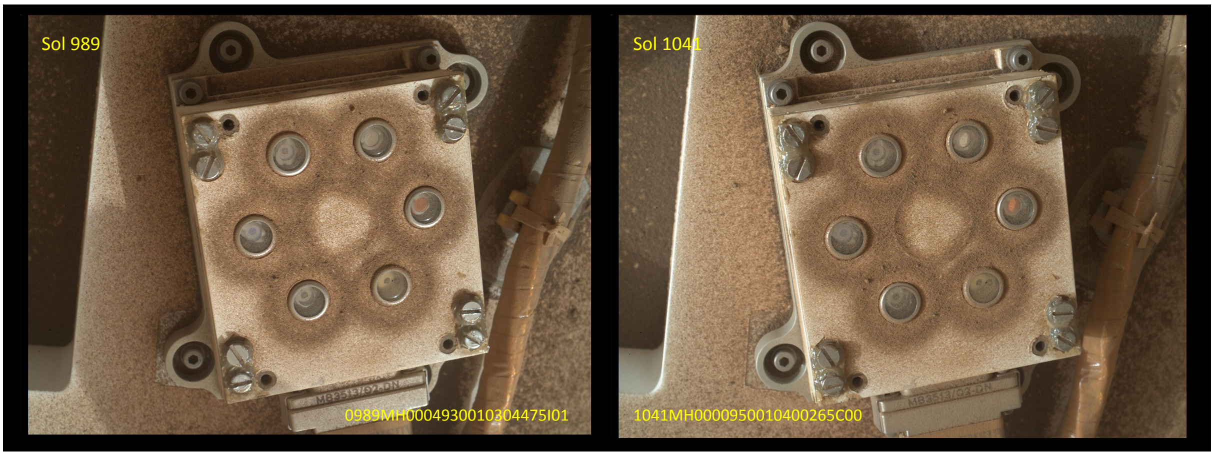


Figure 12. Comparison of the state of the REMS UV sensor between sols 36 and 1041. Note that the time of day at which each image was taken varies. On a 60-sol cadence, MAHLI images the REMS UV sensor to monitor dust coverage over this zenith-looking sensor. MAHLI was also employed to image REMS boom 1 on the RSM to look for signs of damage on the boom that may have occurred during landing and led to the failure of the boom 1 wind sensor.

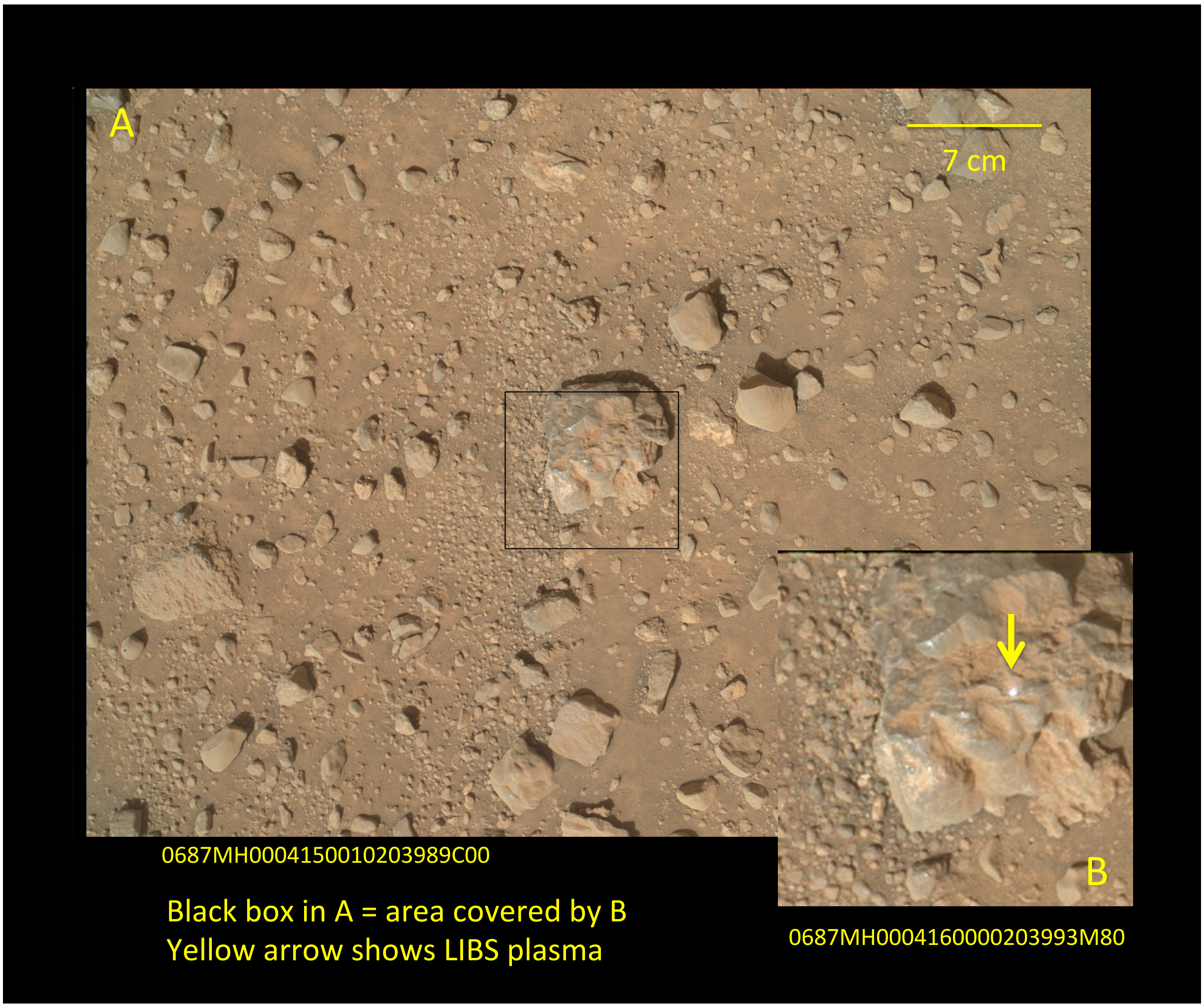


Figure 13. MAHLI images of the target Nova, acquired from 1 meter distance on sol 687, recording conditions before (A) and after (B) removal of dust by the LIBS instrument. LIBS was timed to fire at the same time the image was acquired, allowing the instrument team to capture the laser in action.

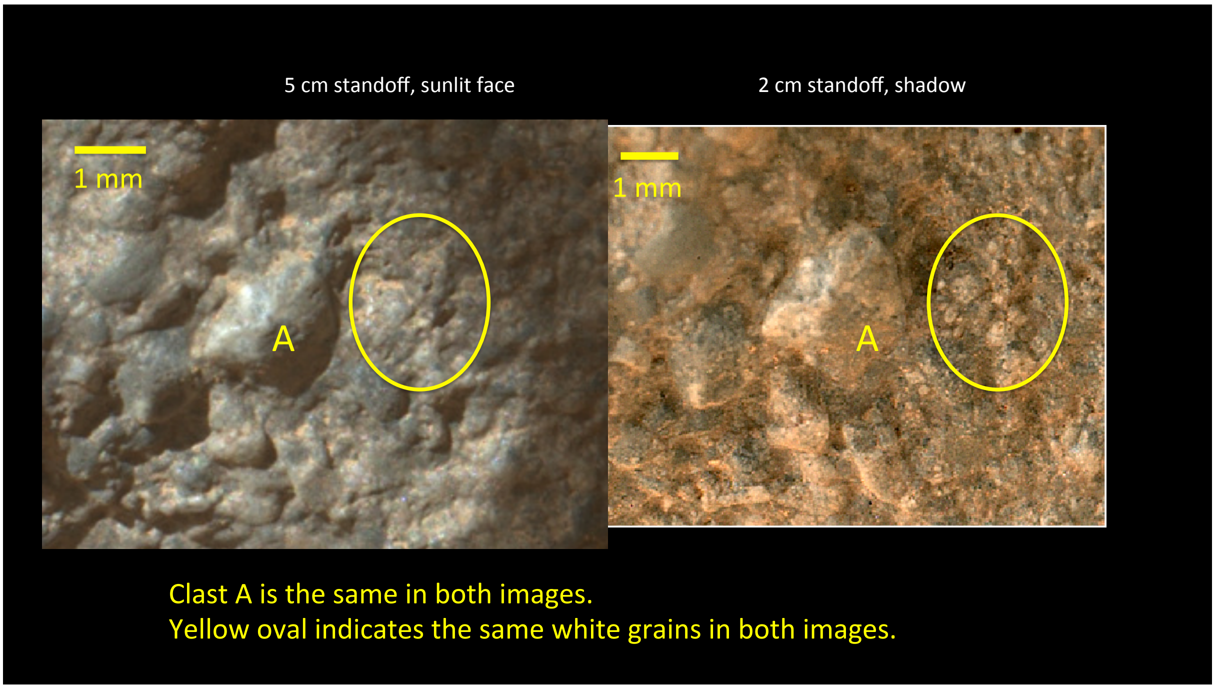


Figure 14. Images of the target Bardin Bluffs acquired in sun (left) and shadow (right). Resolution is slightly different for each image. In full sunlight, the smoothness of clast A results in specular reflections, and grain boundaries are difficult to identify on flatter regions of the rock. The sunlit face is ideal for discriminating grain shape and rock surface morphology. Considerably more color information is available in the shadowed image than the sunlit image.  Individual white grains can be distinguished in the shadowed image, but not in the sunlit face.